Sideband structure in angle-resolved electron spectra from laser-assisted Auger decay generated by ultra-short pulses

2009 J. Phys. B: At. Mol. Opt. Phys. 42 121002

(http://iopscience.iop.org/0953-4075/42/12/121002)

J. Phys. B: At. Mol. Opt. Phys. **42** (2009) 121002 (6pp) doi:10.1088/0953-4075/42/12/121002

FAST TRACK COMMUNICATION

Sideband structure in angle-resolved electron spectra from laser-assisted Auger decay generated by ultra-short pulses

A K Kazansky[1,2] **and N M Kabachnik**[3,4]

[1] Fock Institute of Physics, State University of Sankt Petersburg, Sankt Petersburg 198504, Russia
[2] Donostia International Physics Center, E-20018 San Sebastian/Donostia, Basque Country, Spain
[3] Institute of Nuclear Physics, Moscow State University, Moscow 119991, Russia
[4] Institut für Experimental Physik, Universität Hamburg, 22761 Hamburg, Germany

Received 3 May 2009, in final form 19 May 2009
Published 1 June 2009
Online at stacks.iop.org/JPhysB/42/121002

Abstract
A quantum mechanical model for laser-assisted Auger decay based on the numerical solution of a system of non-stationary Schrödinger equations is developed. The model is applied to a particular case of Ne KLL Auger transitions. The effect of an intense laser field on the angle-resolved spectra of Auger electrons generated by ultrashort (subfemtosecond) pulses is investigated. We demonstrate that for energetic Auger electrons the sideband structure, which appears due to interaction of electrons with the strong laser field, does not correspond to the generally accepted picture of regular equidistant peaks separated by the laser photon energy. Moreover, the structure strongly depends on the observation angle. The origin of this phenomenon is discussed, and it is demonstrated that the standard sideband picture appears after integration over all angles. The described structure can provide a useful tool for controlling the phase of the x-ray pulse relative to the laser pulse in laser-assisted Auger emission experiments.

(Some figures in this article are in colour only in the electronic version)

1. Introduction

When Auger decay of an atom occurs in a strong laser field, the emitted Auger electron interacts with the field, and its energy can change due to absorption or emission of an integer number of photons from the field. Thus, sidebands appear for any Auger line. This phenomenon, known as a laser-assisted Auger decay (LAAD), was first observed by Schins *et al* [1] for LMM Auger transitions in argon. In that and the followed paper [2], the Auger spectra were measured by an electron spectrometer of the magnetic bottle type and therefore those were angle-integrated measurements. The measured spectra consisted of a central (unperturbed) line and a number of sidebands separated by the laser photon energy. The intensity of the sidebands decreased regularly with the number of excess photons. Theoretically this structure was explained on the basis of the strong field approximation [2, 3].

With the advent of attosecond measurements, direct investigation of the time evolution of Auger decay has become possible. In the first experiments [4, 5], the intensity of a sideband of an Auger line in the MNN spectrum of Kr has been measured as a function of the delay time between an exciting subfemtosecond extreme ultraviolet pulse and a strong few-cycle pulse of infrared (IR) laser. The Auger electrons have been detected along the direction of the linear polarization of both pulses. These measurements have stimulated theoretical investigations [6–8] in which the laser-assisted autoionization and Auger decay induced by ultra-short pulses have been considered within the strong field approximation or with a schematic model. However, to the best of our knowledge, the angular distribution of sidebands in LAAD has not been investigated so far, neither theoretically nor experimentally.

In the present work we consider the LAAD within an approach based on a numerical solution of a coupled system of non-stationary Schrödinger equations with realistic atomic potentials. The advantage of our approach is that it permits us to consider both Auger electron and photoelectron spectra including the case when the photon energy is close to the inner-shell threshold. We concentrate our attention on the sideband structure of an Auger line in the angle-resolved Auger spectrum. As an example, we calculate the spectrum of LAAD for KLL transitions in an Ne atom ionized by ultra-short x-ray pulse. This example may be interesting for experimental investigation at the Linac coherent light source (LCLS) which will provide photons with energy sufficient to ionize the 1s shell in Ne [9], and also for future projects at the extreme light infrastructure (ELI) [10].

2. Theoretical approach

In our previous works [11–13] we have developed a non-stationary theory of short-pulse photoionization of inner atomic shells with simultaneous Auger decay of the produced vacancy. For treating LAAD we have to incorporate the interaction of both photo- and Auger electrons with the strong laser field into this theory. In the considered example the x-ray photon energy is not far above the inner-shell threshold; therefore the photoelectron is slow (several eV). It strongly interacts both with the laser field and with the ionic core. We take into account these interactions explicitly by introducing them into the time-dependent Schrödinger equation [14, 15]. In contrast, the Auger electron is very fast (about 800 eV in the Ne case). To a good approximation, its interaction with the laser field may be considered within the strong field approximation [16]. After the decay, the direct interaction of the two ejected electrons can be ignored due to the large difference in their energies. A detailed description of the theory and a derivation of the basic equations will be given elsewhere. Here we only present them in the final form and explain the notations.

The system of non-stationary Schrödinger equations in the case of Auger decay in the strong field of the laser pulse may be written as

$$\mathrm{i}\frac{\partial\phi_d(\vec r,t)}{\partial t} = \left[\hat H_1(\vec r) - \mathrm{i}\frac{\Gamma}{2} - z\mathcal{E}_L(t)\right] \times \phi_d(\vec r,t) - z\mathcal{E}_X(t)\phi_0(\vec r)\,\mathrm{e}^{-\mathrm{i}\varepsilon_0 t}, \quad (1)$$

$$\mathrm{i}\frac{\partial\phi_\epsilon(\vec r,t)}{\partial t} = \left[\hat H_2(\vec r) - E_A + \tfrac{1}{2}[\vec k_A - \vec A_L(t)]^2 - z\mathcal{E}_L(t)\right] \times \phi_\epsilon(\vec r,t) + V\phi_d(\vec r,t). \quad (2)$$

(Here and in the following the atomic units are used unless otherwise indicated.) The system is written for the conditions when both laser and x-ray beams are linearly polarized along the same direction, and the polarization axis is chosen as the z-axis of the coordinate system. The first equation describes a photoexcited electron in the field of the initial vacancy. Here $\hat H_1(\vec r)$ is the Hamiltonian containing the kinetic energy and the local potential felt by this electron, Γ is the width of the vacancy state, $\mathcal{E}_L(t)$ is the IR laser electric field, $\mathcal{E}_X(t)$ is the field of the x-ray pulse, $\phi_0(\vec r)$ and ε_0 are the wavefunction and the energy of the initial state, respectively. The second equation describes the emitted photoelectron in continuum after the Auger decay. Here $H_2(\vec r)$ is the Hamiltonian which contains the interaction of the photoelectron with the residual doubly ionized ion; V is the Auger decay matrix element, $\Gamma = 2\pi|V|^2$; E_A is the energy of a diagram Auger line, $\vec k_A$ is the wave vector of the Auger electron, while $\epsilon = k_A^2/2$ is its energy; $\vec A_L(t) = \int_t^\infty \mathcal{E}_L(t')\mathrm{d}t'$ is the vector potential of the laser field. Equation (2) actually represents a series of equations for $\phi_\epsilon(\vec r,t)$ with different values of ϵ which span the relevant energy interval, while the direction of the Auger electron momentum is fixed.

After solving numerically equations (1) and (2) one can calculate the amplitude of the process as it is described in [11] and finally obtain the four-fold differential cross section. The double differential cross section with respect to the Auger electron energy and emission angle is obtained by integration over the energy and the direction of emission of the photoelectron. The system of coupled equations (1) and (2) describes a variety of phenomena in LAAD including the post-collision interaction in the Auger decay and streaking of photo- and Auger electrons in the laser field. In this paper we restrict our consideration to the sideband structure in Auger electron spectra as obtained from the solution of the system.

3. Results and discussion

As an example, we consider photoionization of the 1s state in the Ne atom with the following KLL Auger decay. The 1s threshold in Ne is 870.1 eV [17] and the strongest line in the Auger spectrum is at 804.3 eV [18]. Since the Auger electron is fast, the described theory may be applied. The measured Auger width of the 1s vacancy is 270 meV [19], which corresponds to the life-time of $\tau = 2.4$ fs. The calculations have been done for the excess energy of 1 Ry, the laser intensity is 10^{12} W cm^{-2}, the laser wavelength is 800 nm, the duration of the IR pulse is 5 fs (FWHM of the field), the duration of the XUV pulse is 330 as. The delay time between the pulses was chosen to be 1.3 fs (the maximum of the IR pulse comes before the maximum of the x-ray pulse). This delay time corresponds to an extremum of the IR field and thus it is close to the zero of the vector potential.

The calculated Auger electron spectrum for the emission of electrons along the polarization direction of the pulses is shown in figure 1 as a solid line. The spectrum consists of a sharp line at the energy corresponding to the undistorted Auger line (∼30 au) and a series of maxima of lower intensity. The sharp line appears owing to those Auger electrons which are emitted after the end of the IR pulse. The shape and the width of this peak correspond to the unperturbed Auger line. In our example the ionization occurs about 3 fs before the end of the IR pulse, while the life-time is 2.4 fs, therefore many electrons are emitted after the pulse. The intensity of this line depends on the delay time and may be used as an independent method for measuring the relative position of the maxima of the two pulses in time. The broad maxima at larger and smaller energies appear due to interaction with the laser field. However, they

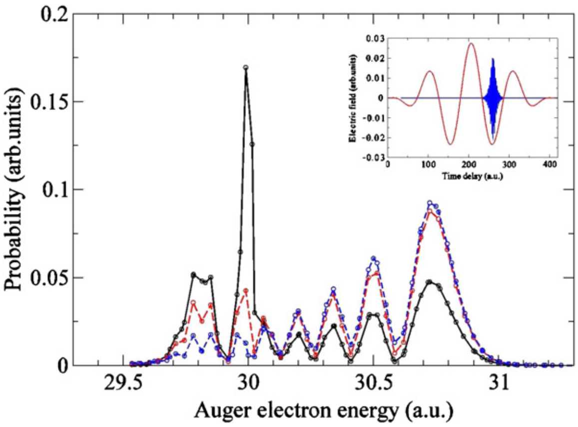

Figure 1. Auger electron spectra for the KLL laser-assisted transition in Ne, $\tau = 2.4$ fs (solid black line). Dashed lines show the same spectra but calculated for shorter life-times, $\tau = 0.8$ fs (long-dashed red line) and $\tau = 0.48$ fs (short-dashed blue line). Auger electrons are emitted in the forward direction, along the laser electric field vector (see the text). Circles show the calculated points, and lines are drawn to guide the eyes. In the inset the relative position of the 5 fs laser pulse (red) and the 330 as x-ray pulse (blue) is shown.

do not look like the usual sidebands. The distance between maxima is larger than 1.6 eV (the energy of the laser photons) and it increases with energy. Besides, the intensity distribution is opposite to the usual intensity distribution of sidebands. The whole spectrum is strongly asymmetric.

In order to understand the origin of this structure, we made calculations for hypothetical shorter life-times of the vacancy. Figure 1 shows the calculated spectra for $\tau = 0.8$ fs and 0.48 fs (dashed curves). One can see that the sharp peak gradually disappears since in these cases practically all Auger electrons are emitted during the IR pulse, but the sideband-like structure preserves and even increases in intensity. Moreover, the positions of the minima do not change. The results for even shorter life-times ($\tau = 240$ as, 160 as, 120 as and 80 as) are shown in figure 2(a). The general character of the spectrum is quite robust, but as the life-time is decreased the minima become shallower and finally disappear for a very short life-time (80 as). In the latter case the decay occurs so fast that the Auger electrons appear practically in the same time interval as photoelectrons which is shorter than the half period of the IR field. This case corresponds to the streaking conditions [20, 21]. The broad maximum in the spectrum corresponds to the Auger-electron pulse broadened and shifted by the laser field. At first sight, a rather large shift of the maximum from the unperturbed position by 0.5 au looks surprising, since the excitation time was chosen near the zero of the vector potential of the IR field. In this case, photoelectron maximum is not shifted but only broadened by the field [20, 21]. However, one should take into account that some Auger electrons are emitted with a delay more than $\tau = 80$ as. In fact, if in the calculations we diminish the life-time even further, the shift of the maximum becomes smaller and smaller. Besides, as it follows from a simple classical picture of the streaking [20], the energy shift is proportional to the square root of electron kinetic energy, which is very high in our case. Thus the observed large shift can easily be explained. Returning to the other curves in figure 2(a), we can interpret the spectra for larger life-times as a combination of streaking and interference of electron waves, emitted at different phases of the IR pulse, but having the same final energy. This leads to the interference pattern superimposed on the streaked peak. A similar structure can be expected for photoelectrons, if the exciting x-ray pulse is sufficiently long [22].

To further investigate the observed structure, we compare our results with the results obtained using the approximate analytical expression for the laser-assisted Auger spectrum presented in [6]. This expression was derived within the strong-field approximation for both photo- and Auger electrons for the infinitely long IR pulse. With slight modification of the original expression and with adjustment of notations, the amplitude of the Auger-electron emission may be written as

$$A_f(\vec{k}_x, \vec{k}_A) \sim \sum_{n=-\infty}^{\infty} i^n J_n\left(\frac{k_A A_0 \cos\theta}{\omega}\right) \times \exp[\mathrm{i}n\omega\Delta t] s(\epsilon_x, \epsilon_A + n\omega). \quad (3)$$

Here $\vec{k}_x$ and $\vec{k}_A$ are the wave vectors of photo- and Auger electrons, respectively, $\epsilon_x = k_x^2/2$ and $\epsilon_A = k_A^2/2$ are the corresponding energies, $J_n(x)$ are the cylindrical Bessel functions, θ is the emission angle of Auger electron relative to the laser polarization vector, A_0 is the amplitude of the vector potential of the laser field, ω is the frequency of this field, Δt is the delay time, and the shape function $s(\epsilon_x, \epsilon_A)$ is

$$s(\epsilon_x, \epsilon_A) = \frac{\tilde{\mathcal{E}}_0(\epsilon_x + \epsilon_A - E_A - \epsilon_0 - \Omega)}{\epsilon_A - E_A + i\Gamma/2}. \quad (4)$$

Here $\tilde{\mathcal{E}}_0$ is the Fourier transform of the envelope of the x-ray pulse and Ω is its carrier frequency. In expression (3) we have omitted the dipole and the Auger matrix elements, since they weakly depend on the energy and do not strongly influence the shape of the spectrum. The latter is mainly determined by the sum of the Bessel functions including the interference between them. The simplified expression (3) depends only on the energy of photoelectron but not on its emission angle. The spectra, calculated using expression (3), are shown in figure 2(b) for exactly the same conditions as the corresponding spectra in panel (a). (We have slightly shifted the energy scale in order to have the same position of the maxima as in figure 2(a).) One can see that both calculations give rather similar results. The position of maxima and minima in spectra agrees very well. Our spectra for a short IR pulse are, naturally, broader than predicted by expression (3) derived for an infinitely long pulse.

The spectra for the laser-assisted Auger emission for different emission angles are shown in figure 3. Panel (a) contains the results of calculations using equations (1) and (2) for a 5 fs IR pulse, panel (b) shows the results of calculation according to analytical expression (3) for a long laser pulse. Both calculations have been done for a hypothetical life-time of the vacancy of 0.5 fs. Qualitatively the spectra calculated within the two models are rather similar. The character of the Auger spectrum drastically changes with the angle. When an Auger electron is emitted perpendicular to the IR field

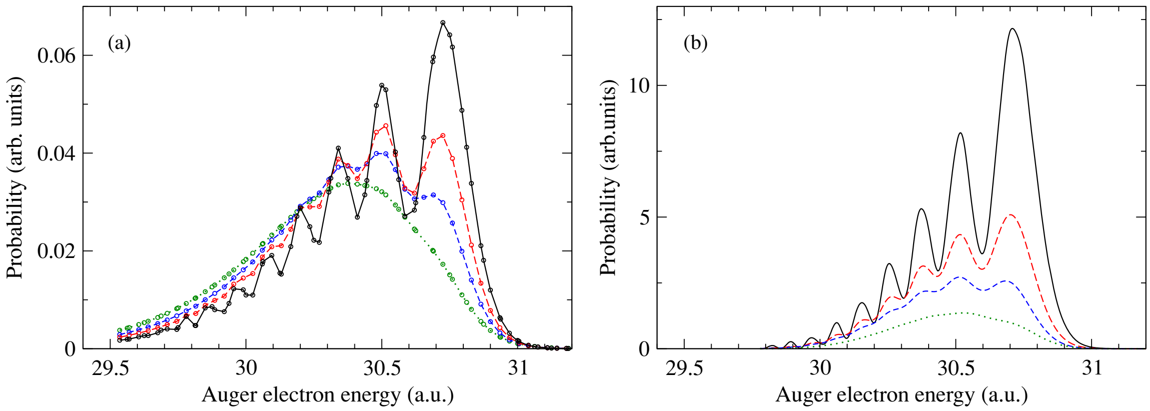

Figure 2. Spectra of Auger electrons emitted in the forward direction along the laser polarization vector, calculated for different hypothetical life-times of the vacancy: $\tau = 240$ as (solid black line), $\tau = 160$ as (long-dashed red line), $\tau = 120$ as (short-dashed blue line) and $\tau = 80$ as (dotted green line). (a) Calculations by solving the TDSE for a short laser pulse. (b) Calculations according to expression (3) for an infinitely long laser pulse.

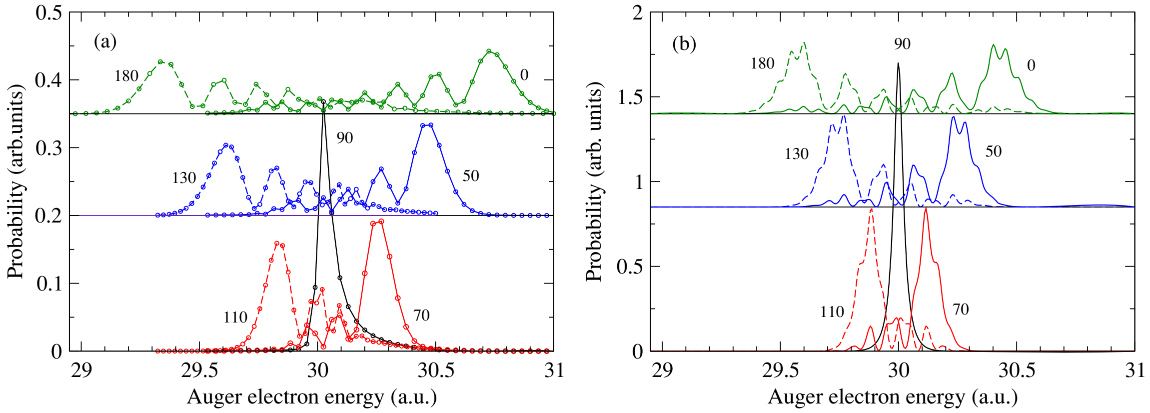

Figure 3. Auger electron spectra for different emission angles indicated at the curves. The spectra were calculated for a hypothetical life-time of the vacancy: $\tau = 500$ as. Solid lines show emission in the forward hemisphere, dashed lines, in the backward hemisphere. (a) Calculations by solving the TDSE for a short laser pulse. (b) Calculations according to expression (3) for an infinitely long laser pulse. The ordinates of the spectra at 0°, 180°, 50° and 130° are shifted for better presentation.

polarization, $\theta = 90°$, the field does not affect its motion, the calculated spectrum has the shape of the laser-unperturbed Auger line. In the case shown in panel (a), this shape includes the post-collision interaction effects. As the emission angle decreases (in the forward hemisphere) the main maximum shifts to higher energies (streaking) and the structure appears. The number of the structure peaks increases with decreasing angle. The picture in the backward hemisphere is almost mirror-symmetrical with respect to the forward hemisphere. It is worth noting that for the infinite IR pulse the fine structure of maxima appears with a typical interval of 1.6 eV. This fine structure is smeared out in the calculations for a short pulse.

One can see from expression (3) that, in general, interference pattern depends on the phase relations between the pulses and, presumably, also on their chirp. Therefore, a study of the sidebands and their angular dependence can be used for the characterization of the pulses. Another interesting conclusion which follows from this expression is that the sideband structure should be (almost) symmetrical with respect to the transformation $\theta \rightarrow \pi - \theta$. This transformation is equivalent to the phase shift of the laser field by π/ω. The symmetry is not exact, it is broken by energy dependence of the dipole and Auger matrix elements which we omitted in expression (3), but approximately it is preserved as it follows from our exact calculations (see figure 3(a)).

If one integrates the double differential cross section over all emission angles, the resulting spectrum shows all typical features of the LAAD with sideband structure. In figure 4 we show the angle-integrated spectrum (solid line) obtained for the case, presented in figure 3(b). Dashed lines show the spectra at some particular angles. One can see a symmetrical picture with a large central maximum and equidistant peaks separated by 1.6 eV. The intensity of the sidebands regularly diminishes as the number of absorbed laser photons increases.

The similarity between the results of the numerical solution of equations (1) and (2) and of the simple analytical approximation (3) makes the latter a useful tool for qualitative

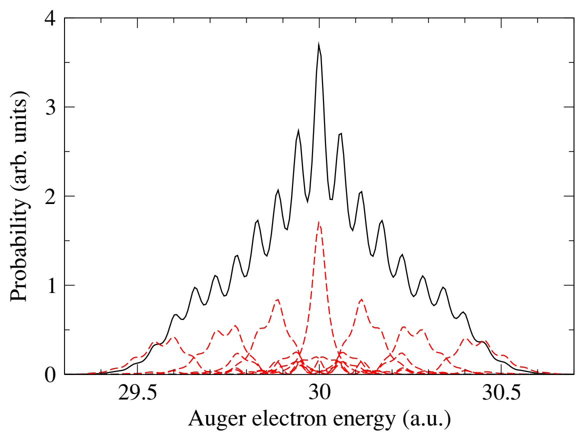

Figure 4. Auger electron spectra calculated for different emission angles (dashed red lines) and the angle-integrated spectrum (solid black line).

consideration. In particular, if the x-ray pulse is long, its Fourier transform is rather sharp, and the shape function (4) is non-zero only in narrow energy intervals around each sideband. In this case, the sidebands do not interfere and the spectrum will consist of lines (almost) symmetrically distributed around the central peak with intensity proportional to the $|J_n|^2$ [6]. This happens when $1/\tau_X \ll \omega$ where τ_X is the duration of the x-ray pulse. In our example of 800 nm laser ($\omega = 1.6$ eV) this situation occurs when $\tau_X \gg 0.5$ fs. For long x-ray pulses the sideband structure does not contain phase information. This is the same for any time delay and therefore it may be observed with non-phase-stabilized lasers. It is interesting that even in this case the angular dependence of the sideband structure will be non-trivial. For large Auger electron energy and large laser intensity, the argument $(k_A A_0 \cos\theta)/\omega$ of Bessel functions in equation (3) may be large. It strongly varies from the maximal value to zero with variation of emission angles from 0° to 90°. This variation leads to systematic disappearance and reappearance of particular sidebands, i.e. to a strong dependence of the sideband intensity distribution on the emission angle.

Similarly, if the Auger decay is very slow (very small width Γ), so that $\Gamma \ll \omega$, due to the resonant denominator in the shape function (4) only narrow energy intervals around each sideband contribute to the spectrum. Also in this case the spectrum of LAAD at any angle is almost symmetrical with respect to the unperturbed line position being independent of any phase relations between the pulses, but it nevertheless strongly depends on the emission angle.

4. Conclusions

In conclusion, we have developed a theoretical approach to the description of the sideband structure in LAAD, based on the numerical solution of the system of non-stationary Schrödinger equations. The calculations for a particular case of KLL Auger decay in Ne have shown that the sideband structure of electron spectra in LAAD strongly depends on the emission angle. For large energy of Auger electrons the angle-resolved spectrum is very asymmetric. If the duration of the laser pulse is comparable with the life-time of the Auger decay, the sideband structure can be used for the determination of the relative phase-shift of the exciting pulse and the laser pulse. The angle-integrated electron spectrum reveals all typical features of the sideband structure in LAAD which were observed earlier. Similar peculiarities of the sideband structure should appear for high-energy electrons in laser-assisted photoelectron spectra produced by x-ray pulses with a duration comparable with the period of the laser field.

Acknowledgments

The authors are grateful to M Drescher, A Rudenko, K Ueda and J Ullrich for their interest in this work and many stimulating discussions. We are indebted to U Heinzmann for his support in our work and for use of the computer facilities of his laboratory in the Bielefeld University where part of the calculations were done. AKK gratefully acknowledges the hospitality of Donostia International Physics Center and financial support by Ikerbasque Foundation via the Ikerbasque Fellowship. NMK gratefully acknowledges the hospitality of the Institut für Experimentalphysik, Universität Hamburg and the financial support of the Max-Planck-Institut für Kernphysik, Heidelberg.

References

[1] Schins J M, Breger P, Agostini P, Constantinescu R C, Muller H G, Grillon G, Antonetti A and Mysyrowicz A 1994 *Phys. Rev. Lett.* **73** 2180
[2] Schins J M, Breger P, Agostini P, Constantinescu R C, Muller H G, Grillon G, Antonetti A and Mysyrowicz A 1995 *Phys. Rev.* A **52** 1272
[3] Fiordilino E, Zangara R and Ferrante G 1988 *Phys. Rev.* A **38** 4369
[4] Drescher M, Hentschel M, Kienberger R, Uiberacker M, Yakovlev V, Scrinzi A, Westerwalbesloh Th, Kleineberg U, Heinzmann U and Krausz F 2002 *Nature* **419** 803
[5] Drescher M, Hentschel M, Kienberger R, Uiberacker M, Westerwalbesloh Th, Kleineberg U, Heinzmann U and Krausz F 2004 *J. Electron Spectrosc. Relat. Phenom.* **137–140** 259
[6] Smirnova O, Yakovlev V S and Scrinzi A 2003 *Phys. Rev. Lett.* **91** 253001
[7] Wickenhauser M, Burgdörfer J, Krausz F and Drescher M 2005 *Phys. Rev. Lett.* **94** 023002
[8] Zhao Z X and Lin C D 2005 *Phys. Rev.* A **71** 060702
[9] http://lcls.slac.stanford.edu/
[10] http://www.extreme-light-infrastructure.eu/eli-home.php
[11] Kazansky A K and Kabachnik N M 2005 *Phys. Rev.* A **72** 052714
[12] Kazansky A K and Kabachnik N M 2006 *Phys. Rev.* A **73** 062712
[13] Kazansky A K and Kabachnik N M 2006 *J. Phys. B: At. Mol. Opt. Phys.* **39** L53
[14] Kazansky A K and Kabachnik N M 2007 *J. Phys. B: At. Mol. Opt. Phys.* **40** 2163
[15] Kazansky A K and Kabachnik N M 2007 *J. Phys. B: At. Mol. Opt. Phys.* **40** 3413
[16] Keldysh L V 1965 *Sov. Phys.—JETP* **20** 1307

[17] Hitchcock A P and Brion C E 1980 *J. Phys. B: At. Mol. Phys.* **13** 3269
[18] Albiez A, Thoma M, Weber W and Mehlhorn W 1990 *Z. Phys.* D **16** 97
[19] Coreno M, Avaldi L, Camilloni R, Prince K C, de Simone M, Karvonen J, Colle R and Simonucci S 1999 *Phys. Rev.* A **59** 2494
[20] Itatani J, Quéré F, Yudin G L, Yu Ivanov M, Krausz F and Corkum P B 2002 *Phys. Rev. Lett.* **88** 173903
[21] Kitzler M, Milosevic N, Scrinzi A, Krausz F and Brabec T 2002 *Phys. Rev. Lett.* **88** 173904
[22] Kazansky A K and Kabachnik N M 2006 *J. Phys. B: At. Mol. Opt. Phys.* **39** 5173